

Stage-specific dual function: EZH2 regulates human erythropoiesis by eliciting histone and non-histone methylation

Mengjia Li,^{1*} Donghao Liu,^{1*} Fumin Xue,^{2*} Hengchao Zhang,¹ Qianqian Yang,¹ Lei Sun,¹ Xiaoli Qu,¹ Xiuyun Wu,¹ Huizhi Zhao,¹ Jing Liu,³ Qiaozhen Kang,¹ Ting Wang,¹ Xiuli An^{4#} and Lixiang Chen^{1#}

¹School of Life Sciences, Zhengzhou University, Zhengzhou, China; ²Department of Gastroenterology, Children's Hospital affiliated to Zhengzhou University, Zhengzhou, China; ³Molecular Biology Research Center and Center for Medical Genetics, School of Life Sciences, Central South University, Changsha, China and ⁴Laboratory of Membrane Biology, New York Blood Center, New York, NY, USA

*ML, DL and FX contributed equally as first authors.

#XA and LC contributed equally as senior authors.

Correspondence: L. Chen
lxchen@zzu.edu.cn

X. An
xan@nybc.org

Received: September 5, 2022.

Accepted: March 28, 2023.

Early view: April 6, 2023.

<https://doi.org/10.3324/haematol.2022.282016>

©2023 Ferrata Storti Foundation

Published under a CC BY-NC license



Abstract

Enhancer of zeste homolog 2 (EZH2) is the lysine methyltransferase of polycomb repressive complex 2 (PRC2) that catalyzes H3K27 tri-methylation. Aberrant expression and loss-of-function mutations of EZH2 have been demonstrated to be tightly associated with the pathogenesis of various myeloid malignancies characterized by ineffective erythropoiesis, such as myelodysplastic syndrome (MDS). However, the function and mechanism of EZH2 in human erythropoiesis still remains largely unknown. Here, we demonstrated that EZH2 regulates human erythropoiesis in a stage-specific, dual-function manner by catalyzing histone and non-histone methylation. During the early erythropoiesis, EZH2 deficiency caused cell cycle arrest in the G1 phase, which impaired cell growth and differentiation. Chromatin immunoprecipitation sequencing and RNA sequencing discovered that EZH2 knockdown caused a reduction of H3K27me3 and upregulation of cell cycle protein-dependent kinase inhibitors. In contrast, EZH2 deficiency led to the generation of abnormal nuclear cells and impaired enucleation during the terminal erythropoiesis. Interestingly, EZH2 deficiency downregulated the methylation of HSP70 by directly interacting with HSP70. RNA-sequencing analysis revealed that the expression of AURKB was significantly downregulated in response to EZH2 deficiency. Furthermore, treatment with an AURKB inhibitor and small hairpin RNA-mediated AURKB knockdown also led to nuclear malformation and decreased enucleation efficiency. These findings strongly suggest that EZH2 regulates terminal erythropoiesis through a HSP70 methylation-AURKB axis. Our findings have implications for improved understanding of ineffective erythropoiesis with EZH2 dysfunction.

Introduction

Erythropoiesis is a complex and tightly controlled cellular process that consists of early erythropoiesis, terminal erythroid differentiation, and reticulocyte maturation. During early erythropoiesis, multipotent hematopoietic stem cells proliferate and differentiate into burst-forming unit-erythroid (BFU-E) cells and colony-forming unit-erythroid (CFU-E) cells. During terminal erythroid differentiation, CFU-E cells differentiate into morphologically recognizable proerythroblasts (Pro), basophilic erythroblasts (Baso), polychromatic erythroblasts (Poly), and orthochromatic erythroblasts (Ortho).^{1,2} Over the last few

decades, a growing body of evidence has revealed the critical roles of epigenetic regulators in the modulation of erythropoiesis.³ Epigenetic dysregulation has been found to be tightly associated with the onset and progression of many hematological malignancies characterized by dyserythropoiesis.⁴

Enhancer of zeste homolog 2 (EZH2) is the core component of polycomb repressive complex 2 (PRC2), a protein complex that catalyzes the trimethylation of histone H3 lysine 27 (H3K27me3), which regulates the expression of downstream target genes.¹⁰ In contrast to extensive studies on the function of *Ezh2* in maintaining the self-renewal of hematopoietic stem progenitor cells by sta-

bilizing the chromatin structure^{5,6} and the roles in regulating the quiescent hematopoietic stem cell pool by supporting their proliferation and exhaustion,⁷⁻¹¹ only few studies have been conducted to explore the role of *Ezh2* during erythropoiesis. Previous studies have shown that deletion of EZH2 results in erythroblast impairment accompanied by enhanced apoptosis.^{12,13} It was shown that the stable expression of EZH2 prevents erythroid precursor cell apoptosis by silencing the expression of Bim1 during the *in vitro*-induced differentiation of human fetal liver CD34⁺ hematopoietic stem cells.¹⁴ Furthermore, it has been reported that EZH2 abnormalities are associated with abnormal erythropoiesis in primary myelofibrosis (PMF), which is a hematopoietic stem cell (HSC) disease characterized by aberrant differentiation of all myeloid lineages and profound disruption of the bone marrow niche.¹⁵ Additionally, numerous recent studies have demonstrated that aberrant expression and loss-of-function mutations of EZH2 are tightly associated with the pathogenesis and evolution of various myeloid malignancies characterized by dyserythropoiesis, such as MDS,¹⁶ AML,¹⁷ and MPN.¹⁸ These findings strongly suggest that EZH2 plays critical roles in the regulation of human erythropoiesis. However, the mechanism by which EZH2 modulates human erythropoiesis still remains largely unknown.

In this study, we explored the roles and mechanism of EZH2 in the regulation of human erythropoiesis by combining a short hairpin RNA (shRNA)-based knockdown strategy and treatment with a specific inhibitor to de-functionalize EZH2. We showed that EZH2 deficiency impaired cell growth and delayed differentiation during the early stage of erythropoiesis and induced the generation of cells with abnormal nuclei and decreased enucleation rates during the terminal stage. Integrated analysis of RNA sequencing (RNA-seq) and chromatin immunoprecipitation sequencing (ChIP-seq) revealed that EZH2 catalyzes histone and non-histone methylation in a stage-specific manner. During the early stage, EZH2 deficiency reduced the abundance of H3K27me₃, which in turn, upregulated the expression of various cyclin-dependent kinase inhibitors (CDKI). However, during the terminal stage when histones are released from the nucleus and are degraded, EZH2 deficiency led to decreased methylation of HSP70 accompanied by decrease of aurora kinase B (AURKB). Notably, similar to EZH2 deficiency, AURKB knockdown also caused the generation of cells with aberrant nuclei and a significant decrease of enucleation rate, strongly suggesting EZH2 regulates terminal erythropoiesis via HSP70-AURKB axis. Our findings provide novel insights into the role of EZH2 in regulating human erythropoiesis and have implications in understanding ineffective erythropoiesis associated with EZH2 dysfunction.

Methods

Antibodies

The details of antibody usage are described in the *Online Supplementary Appendix*.

Erythroid differentiation of CD34⁺ cells and small hairpin RNA-mediated knockdown

Primary human cord blood CD34⁺ cells were isolated from mononuclear cells (MNC) obtained using standard density gradient centrifugation, followed by positive selection using CD34⁺ magnetic selective beads system (Miltenyi Biotechnology, Bergisch Gladbach, Germany) according to the manufacturer's protocol.¹ The cell culture details are described in the *Online Supplementary Appendix*. The detailed preparation of lentivirus, and transduction in CD34⁺ cells have been described previously.¹⁹

Flow cytometry analyses of H3K27me₃

For flow cytometry analysis of H3 Lys27 trimethylation, we collected normal erythroid cells cultured on days 7, 11 and 15. Then the cells were fixed with 4% paraformaldehyde at 25°C for 10 minutes (min) and permeabilized with 0.1% Triton X-100 for 10 min. Cells were washed twice in phosphate-buffered saline (PBS) and stained with anti-Lys27-Me₃ antibody (Cell Signaling Technology, 9733S) for 20 min, then incubated with anti-rabbit IgG Alexa fluor 488 (Cell Signaling Technology, 2975) for 20 min, followed by fluorescence-activated cell sorting (FACS) analysis using a BD LSRFortessa™ flow cytometry.²⁰

Drug treatment

The drugs for cell treatment were as follows. Tazemetostat (EPZ-6438, S7128) was purchased from Selleck and was added into cell culture at a final concentration of 0.5 μM and 5 μM. Barasertib (AZD1152-HQPA, AZD2811, S1147) was purchased from Selleck Chemicals dissolved in dimethyl sulfoxide (DMSO), and was used at a final concentration of 2 nM and 10 nM. Adenosine periodate oxidized (AdOx, A7154) was purchased from Sigma-Aldrich and was used at final concentrations of 10 μM and 20 μM.

Protein immunoprecipitation and immunoblotting

Cells (20×10⁶) were collected and lysed with RIPA buffer (#89900, Thermo Fisher Scientific) supplemented with the proteinase inhibitor PMSF (#36978, Thermo Fisher Scientific) for 1 hour. Cell lysates were precleared with magnetic protein A/G beads (#1614833, Bio-Rad) for 1 hour, followed by incubation with protein A/G beads for 2 hours and finally with antibodies (EZH2, HSP70, HSP90, methylated lysine antibody, or isotype control antibody) for 12 hours at 4°C and then washed 5 times with wash buffer (same as lysis buffer). The immunoprecipitation mixture was boiled in SDS sample buffer and separated by 10% SDS-

PAGE, transferred onto a nitrocellulose membrane (#1620177, Bio-Rad), and western blotting was performed following standard protocols.

Mass spectrometry

The protein bands were shown by Coomassie staining. The blue staining was removed from the SDS-PAGE gel and digested for 12 hours at 37°C with 200 ng of modified sequencing grade trypsin (Promega) in 50 mM ammonium bicarbonate buffer containing RapiGest (Waters Corporation). Digested samples were analyzed by high sensitivity liquid chromatography tandem mass spectrometry and Orbitrap fusion Lumos mass spectrometer (Thermo Fisher Scientific). The mass spectrometry proteomics data have been deposited to the ProteomeXchange Consortium via the PRIDE²¹ partner repository with the dataset identifier PXD039069 and PXD039198.

Data analysis

We performed ChIP-seq and RNA-seq and a detailed description of the data analysis is provided in the *Online Supplementary Appendix*.

Results

Expression and subcellular location of EZH2 and H3K27me3 dynamically changed during erythropoiesis

We differentiated cord blood-derived CD34⁺ cells to erythroid cells using a three-step culture erythroid system, as shown in Figure 1A. Although erythropoiesis is a continuous process, it can be divided into two stages: early erythroid development and terminal erythroid differentiation. The cell composition of each cell category and cytoplasm were shown in the *Online Supplementary Figure S1A, B*. In order to investigate the function of EZH2 during human erythropoiesis, we first analyzed the expression level of EZH2 from the transcriptomics data of highly purified populations of erythroid cells from cord blood and peripheral blood at distinct stages of erythropoiesis.²² The expression of EZH2 was increased in late basophilic and polychromatic erythroblasts, but was decreased in orthochromatic erythroblasts during erythropoiesis (*Online Supplementary Figure S2A, B*). It is well known that EZH2 acts as a histone methyltransferase that catalyzes the modification of H3K27me3.¹⁰ We collected cells at days 7, 9, 11, 13, and 15 during the process of erythroid differentiation and detected the protein level of EZH2 and the abundance of H3K27me3 by western blot. As shown in Figure 1B, EZH2 was consistently expressed at all stages of erythroid development, while the abundance of H3K27me3 was gradually decreased. We also used flow cytometry based strategy to check the level of H3K27me3 according to previous works.²⁰ As shown in the Figure 1C, H3K27me3 was

significantly decreased from day 7 to day 15. We further examined the location of EZH2 and H3K27me3 by immunofluorescence and western blotting on days 7, 11, and 15 (Figure 1D, E). Notably, we found that EZH2 was constantly located in the nucleus, but H3K27me3 was gradually released from the nucleus to the cytoplasm. Given that both EZH2 and H3K27me3 are located in the nucleus in early stage erythroid cells, and that H3K27me3 are predominantly present in the cytoplasm, we hypothesize that EZH2 played a critical role in modulating H3K27me3 during the early erythroid development, while EZH2 regulates cellular function in a H3K27me3-independent manner during the terminal erythroid development.

Deficiency of EZH2 impaired cell growth and delayed differentiation in the early stage of erythropoiesis

In order to test our hypotheses, we used two methods to achieve EZH2 dysfunction during early and terminal erythroid development. One strategy used a shRNA-mediated approach using a tetracycline-inducible-GFP expression system that is induced by adding doxycycline (DOX) at specific stages, and the second approach was to treat cells with EPZ6438, a specific inhibitor of EZH2 (Figure 2A). We first determined the knockdown efficiency of EZH2 in the erythroid progenitors using real-time polymerase chain reaction and western blot analysis, which was shown to be nearly 80% (*Online Supplementary Figure S3A–C*). EZH2 deficiency reduced the cell number of the erythroid progenitor cells by 4-fold as compared to that of the control group (Figure 2B). In order to address the causes for impaired cell growth, we examined cell apoptosis using 7-AAD and Annexin V double staining and found that the cell apoptosis rate of the control group and EZH2 knockdown group were approximately 7.29% and 7.51%, respectively. For the DMSO control, the apoptosis rate was 4.91%, while the apoptosis rate of the EPZ6438 0.5 μM and EPZ6438-5 μM groups was 5.98% and 6.0%, respectively (*Online Supplementary Figure S4A*). There was no significant difference in the cell apoptosis rate between the control and EZH2 dysfunction groups (*Online Supplementary Figure S4B*). We then checked cell cycle using an EdU flow cytometry assay and we found that knockdown of EZH2 led to G1 phase cell cycle arrest of erythroid progenitors (Figure 2C). Aside from the impairment of cell growth, we further found that EZH2 knockdown also delayed the differentiation of erythroid progenitor cells with an increase in BFU-E and decreased in CFU-E (Figure 2D). We then checked the colony-forming ability of erythroid progenitors and found that the number and size of BFU-E and CFU-E clones in the control groups were significantly greater than that of EZH2-defunctionalized groups (Figure 2E). In summary, dysfunction of EZH2 impaired cell growth by arresting the cell cycle in G1 phase and delayed differentiation during early erythroid development.

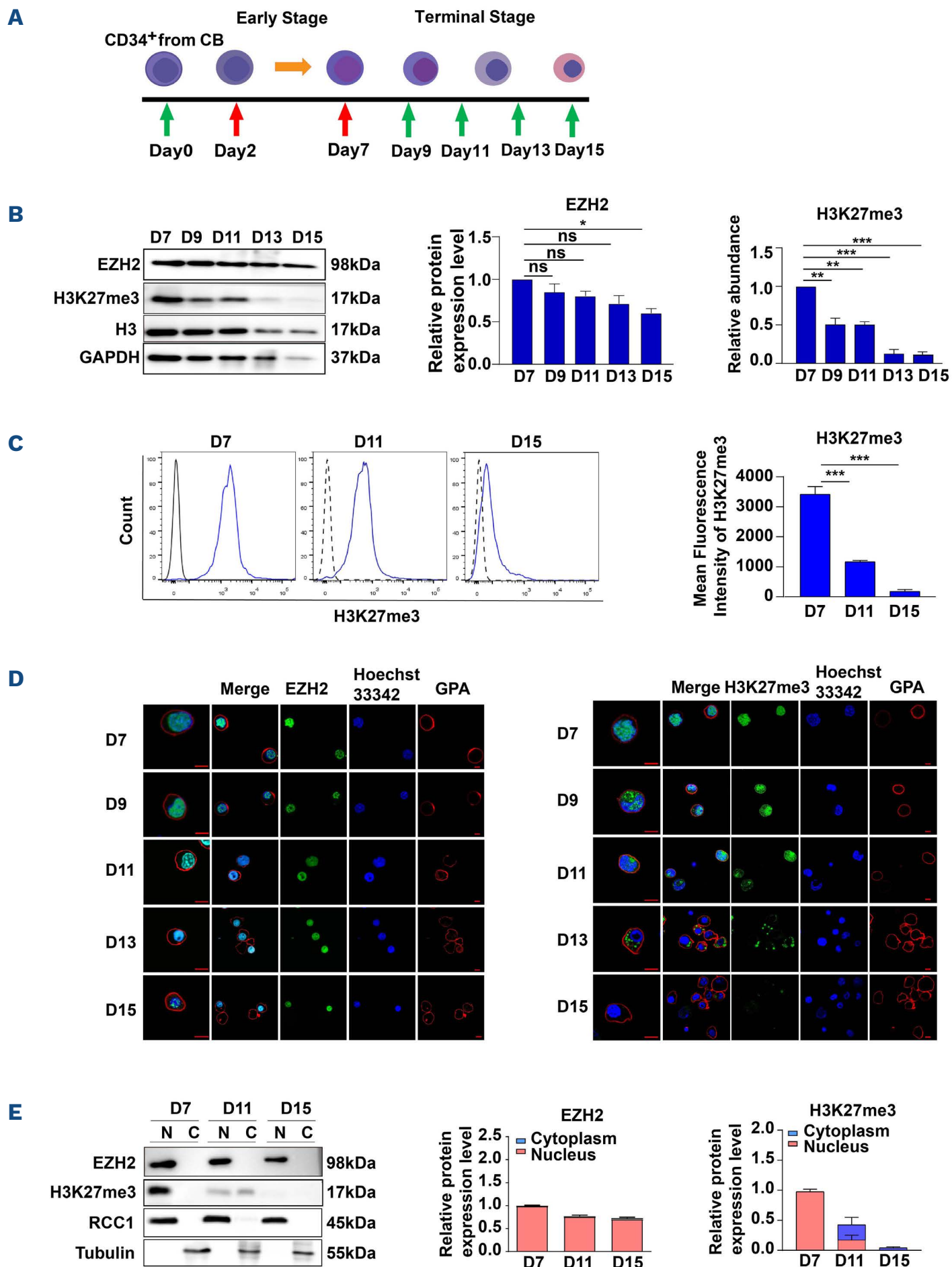


Figure 1. The abundance and localization of EZH2 and H3K27me3 during erythropoiesis. (A) Schematic diagram of erythroid cell differentiation from CD34⁺ cells. The day of getting CD34⁺ cells was recorded as day 0. Early erythroid development was the first phase (day 0 to day 7), terminal erythroid development was the second and third phase (day 7 to day 15). (B) Representative western blot showing the level of EZH2 and H3K27me3 in whole cell lysates prepared from cultured erythroid cells on days 7, 9, 11, 13, and 15. Quantitative analysis of EZH2 and H3K27me3 from 3 independent experiments. The H3K27me3 signals were normalized to H3 using densitometric analysis with ImageJ software. (C) Flow cytometry analysis of H3K27me3 in normal erythroid cells cultured on days 7, 11 and 15. Quantitative analysis from 3 independent experiments showing the abundance of H3K27me3. (D) Immunofluorescence images showing the location of EZH2 and H3K27me3 (green) on days 7, 9, 11, 13, and 15. Hoechst 33342 (blue) was used to stain the nucleus. GPA (red) was used to stain the membrane of terminal erythroid cells. (E) Western blot analysis showing the location of EZH2 and H3K27me3 by extracting nuclear and cytoplasm protein. RCC1 and tubulin were used as nuclear and cytoplasmic markers, respectively. Quantitative analysis of EZH2 and H3K27me3 protein level in the nucleus and cytoplasm from 3 independent experiments. Statistical analysis is from 3 independent experiments, and the bar plot represents mean \pm standard deviation of triplicate samples. ns: not significant; * $P < 0.05$, ** $P < 0.01$, *** $P < 0.001$.

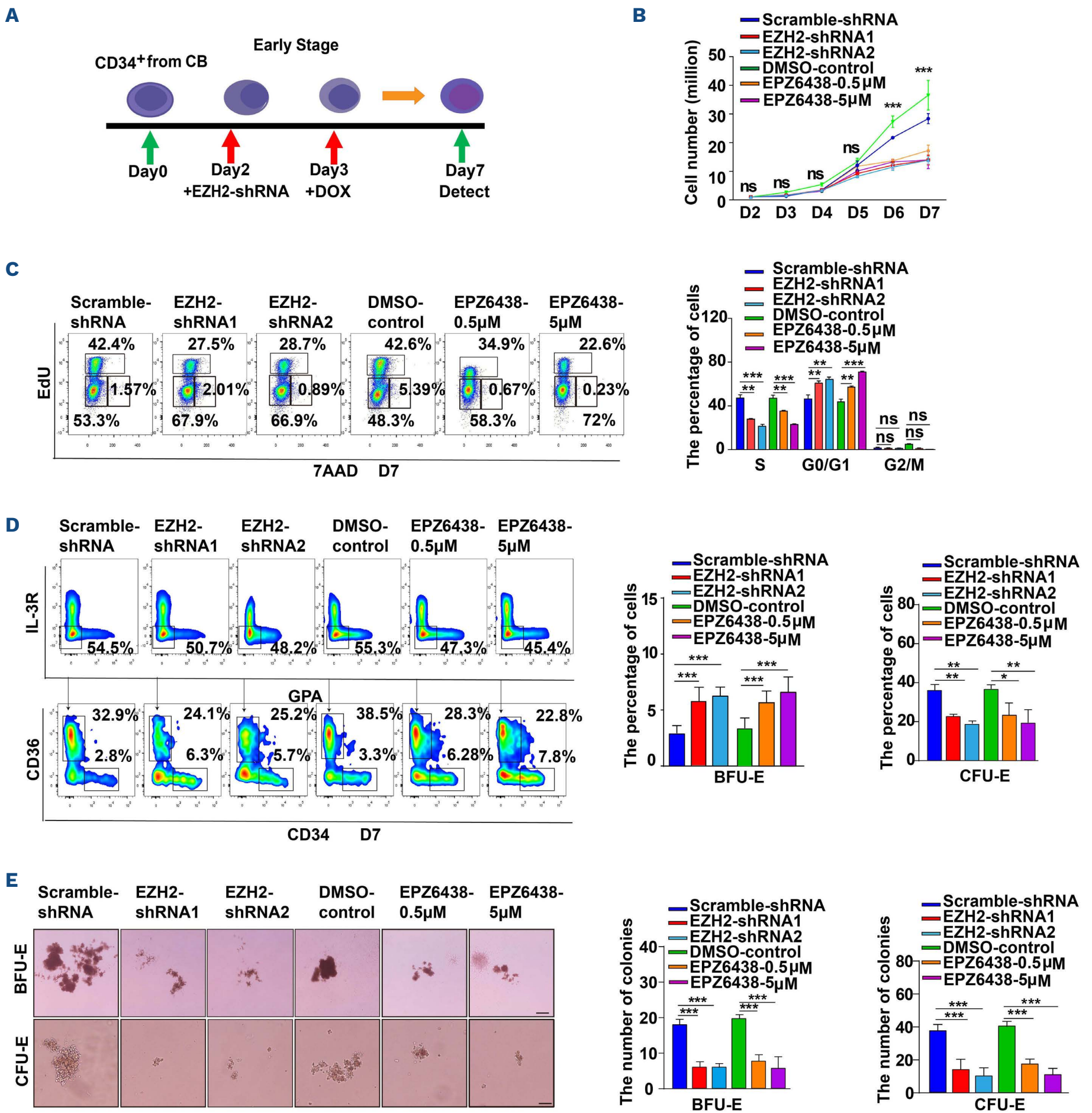


Figure 2. Deficiency of EZH2 impaired cell growth and delayed differentiation during early stage of human erythropoiesis. (A) Schematic diagram of experiment method. The day of getting CD34⁺ cells was recorded as day 0. Lentivirus human CD34⁺ transduction at day 2. During the early stage erythroid development, small hairpin RNA (shRNA)-mediated knockdown was performed by using a tetracycline-inducible-GFP expression system, which can be induced by adding doxycycline (DOX) at day 3 or defunctionalized EZH2 by treating cells with EPZ6438 at day 3. (B) Growth curves of cells, including scramble-shRNA, EZH2-shRNA, dimethyl sulfoxide (DMSO) control, EPZ6438-0.5 μM, and EPZ6438-5 μM. (C) Representative flow cytometry profiles of the cell cycle as assessed by EdU and 7-AAD staining of day 7 erythroid cells. Quantitative analysis of the cell cycle from 3 independent experiments. (D) Flow cytometry analysis of erythroid progenitor cells at day 7. The fold change of absolute progenitor cells (burst-forming unit-erythroid [BFU-E] and colony-forming unit-erythroid [CFU-E]) number. (E) Colony-forming ability of erythroid cells derived from scramble-shRNA, EZH2-shRNA, DMSO control, EPZ6438 0.5 μM, and EPZ6438 5 μM in BFU-E colony medium or CFU-E colony medium on day 6; scale bar, 200 μm. Quantitative analysis the number of BFU-E and CFU-E colonies from 3 independent experiments. Statistical analysis is from 3 independent experiments, and the bar plot represents mean ± standard deviation of triplicate samples. ns: not significant; **P*<0.05, ***P*<0.01, ****P*<0.001.

Integrated chromatin immunoprecipitation sequencing and RNA sequencing analyses of the effect of EZH2 on the early stage of erythropoiesis

In order to further confirm our conjecture and explore the mechanism of EZH2 regulating early erythropoiesis via catalyzing the formation of H3K27me₃, we performed ChIP-seq and RNA-seq analyses of control and EZH2-knockdown erythroblasts cultured for 7 days (*Online Supplementary Figure S5*). Heat maps and corresponding profile plots of ChIP-seq displayed a significant decrease in the abundance of H3K27me₃ in response to EZH2 knockdown (Figure 3A, B). We further conducted genomic feature analysis of the distribution of H3K27me₃, and found that 23.57% of decreased peaks in EZH2-shRNA group had presence in the promoter regions (*Online Supplementary Figure S6A*). Volcano plot and heat map analysis of the RNA-seq data showed that there were approximately 696 differentially expressed genes (DEG) between the scramble-shRNA and EZH2-shRNA groups (adjusted *P* value <0.1), and the number of upregulated and downregulated genes in EZH2-deficient cells was 570 and 126, respectively (*Online Supplementary Figure S6B, C*). Gene ontology (GO) pathway enrichment analysis for DEG revealed that the upregulated genes were mainly enriched in the hemostasis and functional activation of hematopoietic cells, while the down-regulated genes predominantly enriched in metabolic pathways (*Online Supplementary Figure SA, B*). Box plot of integrated ChIP-seq and RNA-seq analysis showed that the upregulated expression of genes was tightly associated with the reduction of H3K27me₃ in EZH2-shRNA group (Figure 3C). Further GO terms analysis showed that the upregulated genes were significantly enriched in the cell growth-associated biological processes, such as negative regulation of growth, negative regulation of cell growth, and cell growth (Figure 3D). Heat maps showed that decreased H3K27me₃ signal around transcription start site (TSS) and upregulated CDK gene expression in EZH2-shRNA group (*Online Supplementary Figure S8A*). Furthermore, the integrated analysis also revealed enrichment peaks of H3K27me₃ at the promoter region of *CDKN1A* and *CDKN1C* (Figure 3E), together with significantly upregulated mRNA expression of *CDKN1A* and *CDKN1C* (approximately 8 times) in EZH2-shRNA group (*Online Supplementary Figure S8B, C*). Taken together, our data show that EZH2 regulates the expression of CDK-related genes by modulating the modification of H3K27me₃ and plays critical roles in the regulation of erythroid progenitor cell growth and differentiation of erythroid progenitors during early erythroid development.

Knockdown of EZH2 induced the generation of abnormal nuclear cells and impaired enucleation during the terminal erythroid development

We then further explored the roles and mechanisms through which EZH2 regulates terminal erythroid devel-

opment (Figure 4A). We first determined the knockdown efficiency of EZH2 of erythroblasts during the terminal stage of erythropoiesis using real-time polymerase chain reaction (PCR) and western blotting. We found that the knockdown efficiency of EZH2 was approximately 85% on days 11 and 15 (Figure 4B-D). By counting cell numbers from day 7 to day 15, we found that the number of cells in the control and EZH2-knockdown groups increased from approximately 1×10^6 to about 100×10^6 , whereas for the control and EPZ6438-treated groups, the cell numbers increased from approximately 1×10^6 to about 130×10^6 (*Online Supplementary Figure S9A*). Then we detected cell apoptosis in the erythroblasts at days 11 and 13 using 7-AAD and Annexin V double-staining, which were analyzed by flow cytometry. The ratio of apoptotic cells in the Scramble-shRNA group increased from approximately 6.7% to 8.9%, as compared to approximately 8.9% to 10.1% in the EZH2-knockdown group. For the control and EPZ6438-treated groups, the ratio of apoptotic cells increased from approximately 5.7% to 8.8% and from approximately 6.4% to 9.4%, respectively. Taken together, we found that dysfunction of EZH2 had no effect on either the cell growth or cell apoptosis (*Online Supplementary Figure S9B, D*). We also monitored changes in the cell cycle by an EdU incorporation assay, and we found no significant difference between the control and experimental groups (*Online Supplementary Figure S9C, E*). The differentiation of CFU-E cells into erythroid precursors is characterized by the surface expression of glycoprotein A (GPA), a specific marker of erythroid cells. The results showed that there was no difference in the ratio of GPA-positive cells on days 9, 11, 13, and 15 (*Online Supplementary Figure S10A, B*). Using $\alpha 4$ -integrin and Band 3 as surface markers, differentiation of pro-erythroblasts to late-stage erythroblasts was detected by flow cytometry. The results showed that dysfunction of EZH2 does not affect terminal erythroid differentiation (*Online Supplementary Figure S10D, E*). Notably, the morphological observations indicated that both EZH2 knockdown and EPZ6438 treatment significantly increased the generation of cells with abnormal nuclei, with approximately 22% and 28% on days 13 and 15, respectively (Figure 4E; *Online Supplementary Figure S10C*). In addition, by using flow cytometry to check the extruded nuclei that were stained with Hoechst 33342, we found that EZH2 dysfunction also caused a dramatic decrease in the enucleation rate to approximately 15% and 20% on days 13 and 15, respectively. However, enucleation rates were approximately 30% and 50% on days 13 and 15, respectively, for the control group (Figure 4F). In conclusion, although dysfunction of EZH2 did not affect cell growth and differentiation, both knockdown of EZH2 and treatment with EPZ6438 led to significant impairment of the terminal stage of erythropoiesis by inducing the generation of erythroblasts with abnormal nuclei, which caused a reduction in the enucleation rate.

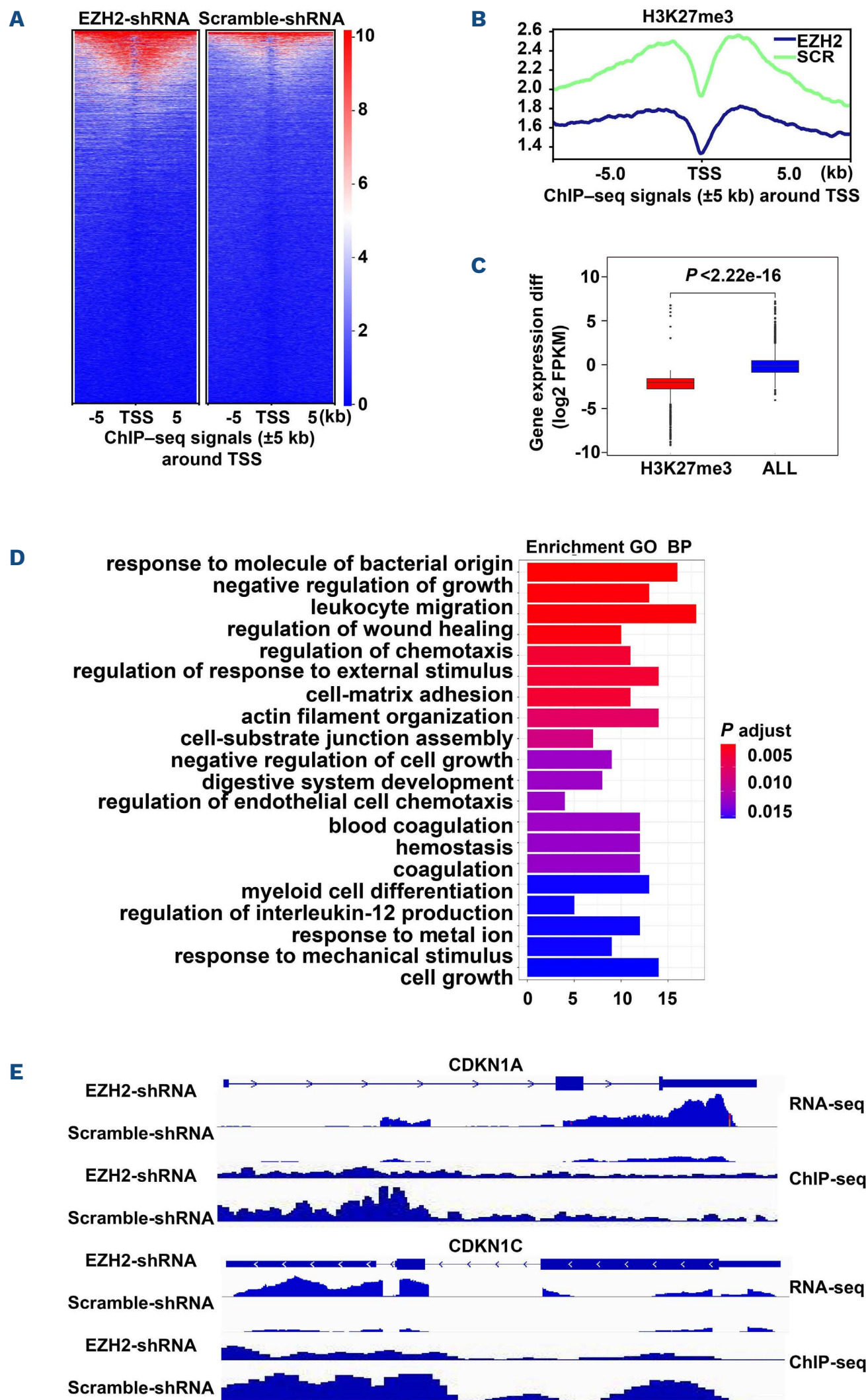


Figure 3. EZH2 regulated the CDK-related genes by modulating H3K27me3 during early stage erythropoiesis. (A) The heat maps showing the chromatin immunoprecipitation sequencing (ChIP-seq) signals of EZH2-small hairpin RNA (shRNA) (left) and scramble-shRNA (right) around TSS. (B) Representative peaks chart image showing the ChIP signals of EZH2-shRNA (blue) and scramble-shRNA (green) around TSS. (C) Box chart analysis showing downregulation of *H3K27me3* gene expression. (D) Go analysis showing the functional classification of upregulation DEG by regulated of *H3K27me3* after knockdown EZH2. (E) Methylation and gene expression level at *CDKN1A* and *CDKN1C* locus in scramble-shRNA and EZH2-shRNA.

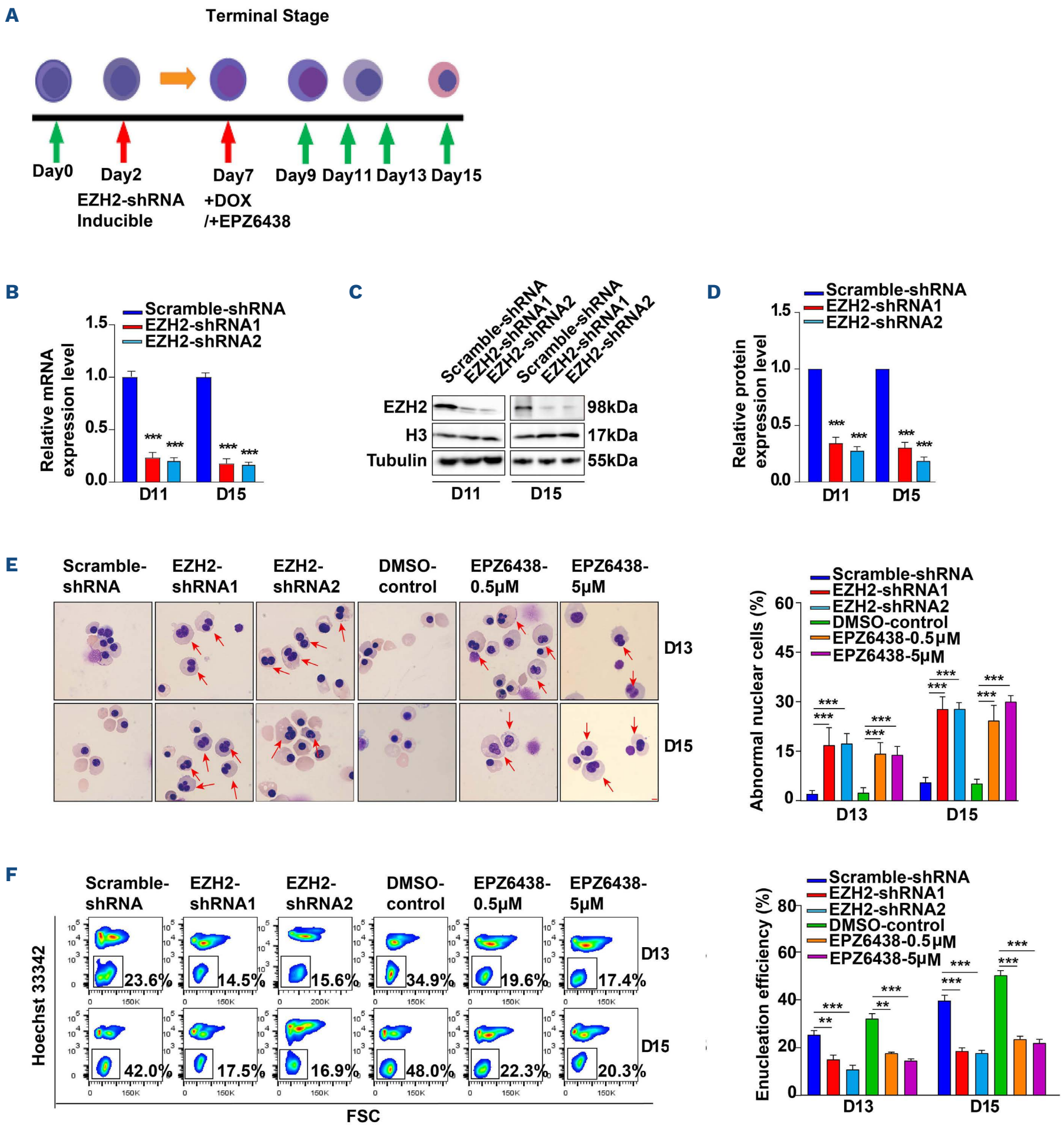


Figure 4. Knockdown of EZH2 induced abnormal nuclear cells and impaired enucleation during terminal erythropoiesis. (A) Schematic diagram of experiment method. The day of getting CD34⁺ cells was recorded as day 0. Lentivirus transduction human CD34⁺ at day 2. Doxycycline (DOX) or EPZ6438 was added at day 7. (B) Quantitative real-time polymerase chain reaction (qRT-PCR) results showing EZH2 expression in erythroblasts infected with lentivirus containing scramble-small hairpin RNA (shRNA) and EZH2-shRNA on days 11 and 15. (C) Representative western blot images showing the knockdown efficiency of scramble-shRNA and EZH2-shRNA on days 11 and 15. (D) Quantitative analysis the knockdown efficiency of EZH2 from 3 independent experiments. (E) Representative images of scramble-shRNA, EZH2-shRNA, dimethyl sulfoxide (DMSO) control, EPZ6438-0.5 µM, and EPZ6438-5 µM on day 15. Red arrow pointed to cells with abnormal nuclear morphology; scale bar, 5 µm. Statistical analysis of abnormal nuclear cells from 3 independent experiments. (F) Flow cytometry analysis showing the enucleation efficiency of scramble-shRNA, EZH2-shRNA, DMSO control, EPZ6438 0.5 µM, and EPZ6438 5 µM on days 11 and 15. Statistical analysis of the enucleation efficiency from 3 independent experiments. Statistical analysis is from 3 independent experiments, and the bar plot represents mean ± standard deviation of triplicate samples. ns: not significant; **P*<0.05, ***P*<0.01, ****P*<0.001.

EZH2 interacted with HSP70 and catalyzed HSP70 methylation

In order to understand the molecular mechanisms underlying EZH2 regulation of terminal erythropoiesis, we carried out a co-immunoprecipitation coupled with mass spectrometry (CoIP-MS) assay to identify proteins that interact with EZH2. As shown in Figure 5A, various non-histone proteins were found to possess the capability to bind with

EZH2, among which HSPA8, HSP90AB1, HSP90AA1, and HSPA1B were identified to have the highest binding capability. Previous studies have reported that HSPA8 and HSPA1B are members of the HSP70 family, which is an evolutionarily conserved family of ATP-dependent chaperones involved in a variety of biological processes.²³⁻²⁵ Both HSP90AB1 and HSP90AA1 belong to the HSP90 protein family, which are highly conserved ubiquitous molecule.^{26,27}

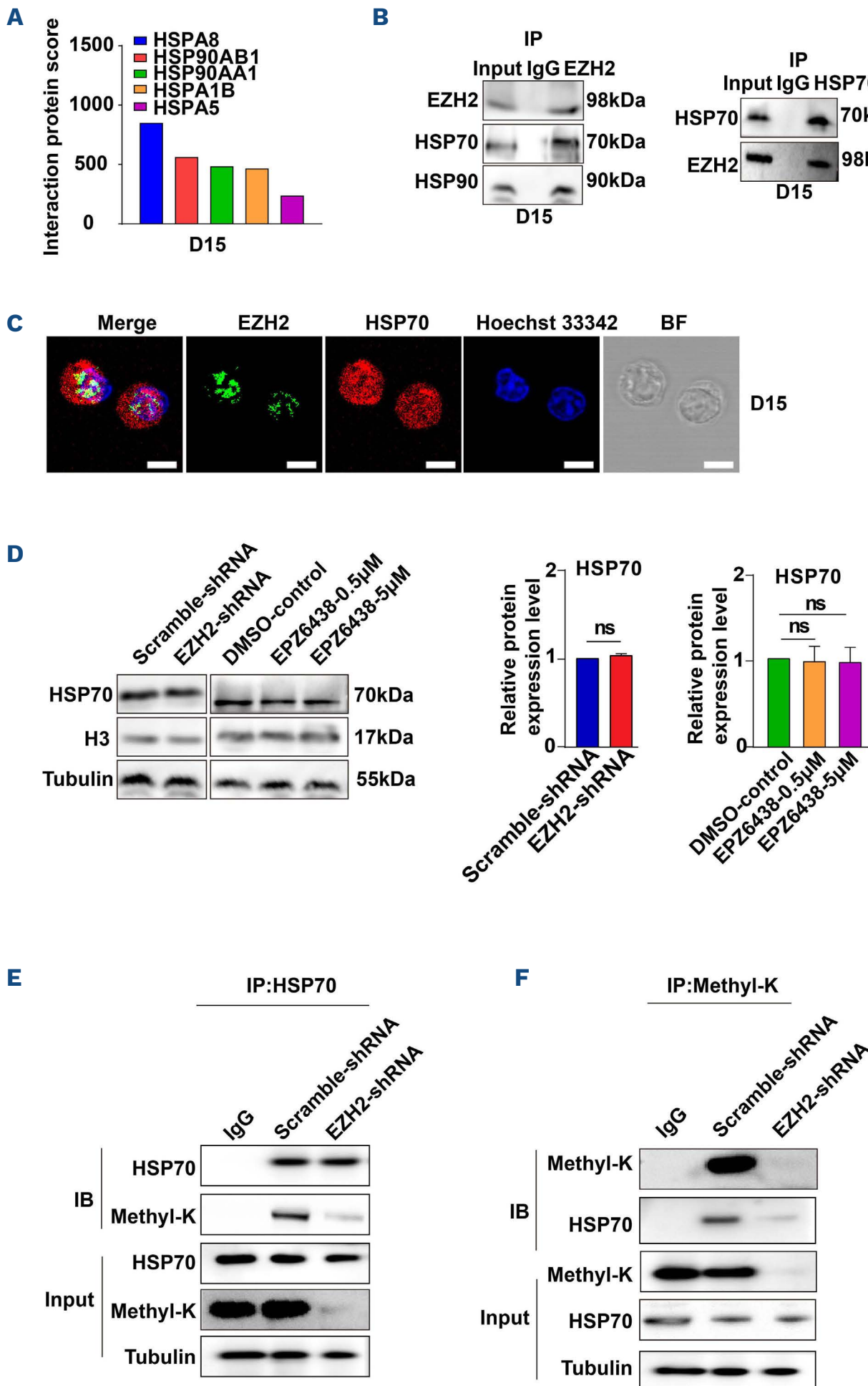


Figure 5. EZH2 interacted with HSP70 and catalyzed HSP70 methylation.

(A, B) Mass spectrometry analysis of proteins pulled-down by an anti-EZH2 antibody. Immunoprecipitation (IP) was performed using cell lysates collected from cultured cells on day 15 using control IgG, anti-EZH2 antibody, or anti-HSP70 and anti-HSP90 followed by immunoblotting (IB) with anti-HSP70 antibody or anti-EZH2 antibody, followed by IB with anti-HSP90 antibody or anti-EZH2 antibody. (C) Immunofluorescence images showing the co-localization of EZH2 (green) and HSP70 (red). Hoechst 33342 (blue) was used to stain the nucleus. (D) Representative western blot showing the protein level of HSP70 in cells transfected with scramble-small hairpin RNA (shRNA) or EZH2-shRNA and treated with or without EPZ6438 (0.5 µM, 5 µM). H3, and Tubulin were used as loading control. Quantitative analysis of the relative protein level of HSP70 from 3 independent experiments. (E, F) IP analysis of anti-HSP70 or anti-Methyl-K was performed followed by IB with anti-Methyl-K or HSP70 in cells were transfected with scramble-shRNA and EZH2-shRNA. Statistical analysis is from 3 independent experiments, and the bar plot represents mean \pm standard deviation of triplicate samples. ns: not significant; * P <0.05, ** P <0.01, *** P <0.001. IgG: immunoglobulin G.

In order to verify the mass spectrometric results, we performed immunoprecipitation with an anti-EZH2 antibody followed by immunoblotting using anti-HSP70 antibody and anti-HSP90 antibodies. The results further confirmed that EZH2 can interact with both HSP70 and HSP90 proteins (Figure 5B). In order to further confirm the interaction between EZH2 and HSP70, we performed immunofluorescence staining to check the location of EZH2 and HSP70. We found that they were co-localized together in the nucleus (Figure 5C). In addition, by checking the expression of HSP70 after knockdown of EZH2, we found that the protein level of HSP70 remained unchanged in the EZH2 dysfunction group as compared to the control group (Figure 5D). Recently, it was reported that EZH2 performs a non-canonical enzymatic role by which EZH2 catalyzes the methylation of specific lysine residues of various non-histones.^{28,29} Thus, we speculated that, by direct binding to HSP70 and HSP90, EZH2 might exert regulatory roles by mediating the methylation of HSP70 or HSP90. By performing immunoprecipitation with a HSP70 or HSP90 antibody followed by immunoblotting using a pan-methyl lysine antibody, we found that dysfunction of EZH2 actually affected the methylation of HSP70, but not HSP90. We performed western blot analysis combined with co-immunoprecipitation to assess the function of EZH2 in HSP70 and HSP90 methylation. We found that HSP70 methylation was attenuated after EZH2 deficiency (Figure 5E, F). However, no methylation of HSP90 was detected (*data not shown*), suggesting that HSP90 methylation was not involved in mediating EZH2 function. In order to gain further evidence that EZH2 catalyzes HSP70 methylation, we sought to identify the potential methylation sites in HSP70 protein by mass spectrometry. As shown in *Online Supplementary Figure S11*, we found that in the control group there were four methylated sites of HSP70, which were Lys7, Lys9, Lys10, and Lys33, while there were no methylated sites observed on HSP70 in the EZH2-knockdown groups. All of these results strongly indicate that EZH2 can bind to HSP70, which thus, modulates the terminal stage of erythropoiesis by catalyzing methylation of HSP70.

Knockdown of EZH2 resulted in downregulation of AURKB at the transcriptional level

In order to further explore the molecular mechanisms underlying the roles of EZH2 in the regulation of terminal erythroid development, we performed RNA-seq analysis on cells in the control and EZH2-knockdown groups on day 15 (Figure 6A). Volcano and heat map analysis showed that the number of DEG were approximately 419, with approximately 166 and 253 genes upregulated and downregulated in EZH2-knockdown cells, respectively (Figure 6B, C). Downregulated genes were enriched with GO terms involved in various biological processes reported to be tightly associated with nuclear condensation and enucle-

ation, which occur specifically during the terminal stage of erythropoiesis,³⁰⁻³² including chromosome segregation, organelle fission and spindle organization. Gene set enrichment analysis (GSEA) revealed that the *AURKB* gene, a subunit of the chromosome passenger protein complex, which ensures accurate chromosome segregation and cell division, was present in most of these key pathways (Figure 6D, E). Based on the occurrence of methylation on non-histone protein HSP70, we speculated that HSP70 methylation was tightly associated with the regulation of the expression of *AURKB* at the transcriptional level. In order to test this, we treated day 14 cells with or without the methyltransferase inhibitor adenosine-2',3'-dialdehyde (AdOx) (2 nM and 10 nM)³³ and then determined the abundance of HSP70 methylation and expression of *AURKB*. Western blot analysis showed that global lysine methylation decreased while the protein expression of HSP70 was unchanged (Figure 7A-C). We then performed an immunoprecipitation experiment using anti-HSP70 antibody or anti-methyl-lysine antibody followed by immunoblotting using an anti-methyl-lysine or anti-HSP70 antibody. As shown in Figure 7D and E, the results showed that HSP70 methylation dramatically decreased in the presence of AdOx. We further found that the transcript level of *AURKB* was also significantly downregulated, which was accompanied with a decrease in the methylation of HSP70 (Figure 7F). In conclusion, the decreased of *AURKB* transcription could be attributed to a reduction of HSP70 methylation.

Dysfunction of AURKB led to the generation of abnormal nucleus and impairment in enucleation efficiency

We then conducted experiments to examine the effects of *AURKB* deficiency on terminal erythropoiesis. We treated day 11 cultured normal cells with AZD2811,³⁴ an *AURKB* inhibitor used at 2 nM and 10 nM or knockdown *AURKB* using shRNA-mediated approach on day 11. Flow cytometry analysis showed that the addition of AZD2811 had no effect on cell apoptosis at days 13 and 15 (*Online Supplementary Figure S12A, B*). Furthermore, there were no difference in terminal erythroid differentiation after adding AZD2811 (*Online Supplementary Figure S12C, D*). However, we found that addition of AZD2811 impaired the enucleation efficiency in cells on days 13 and 15. The enucleation efficiency with AZD2811 treatment was decreased nearly 15% and 28% on days 13 and 15 (Figure 8A, B), respectively. Similarly, knockdown of *AURKB* also decreased enucleation efficiency. Upon morphology observation, approximately 20% of the cells in the AZD2811 groups and *AURKB*-shRNA groups had abnormal nuclei (Figure 8C, D). These results suggested that inhibiting the function of *AURKB* can also cause abnormal nuclei and decreased enucleation efficiency. In summary, these findings suggested that EZH2 may regulated *AURKB* expression by mediating HSP70 methylation during terminal erythroid development.

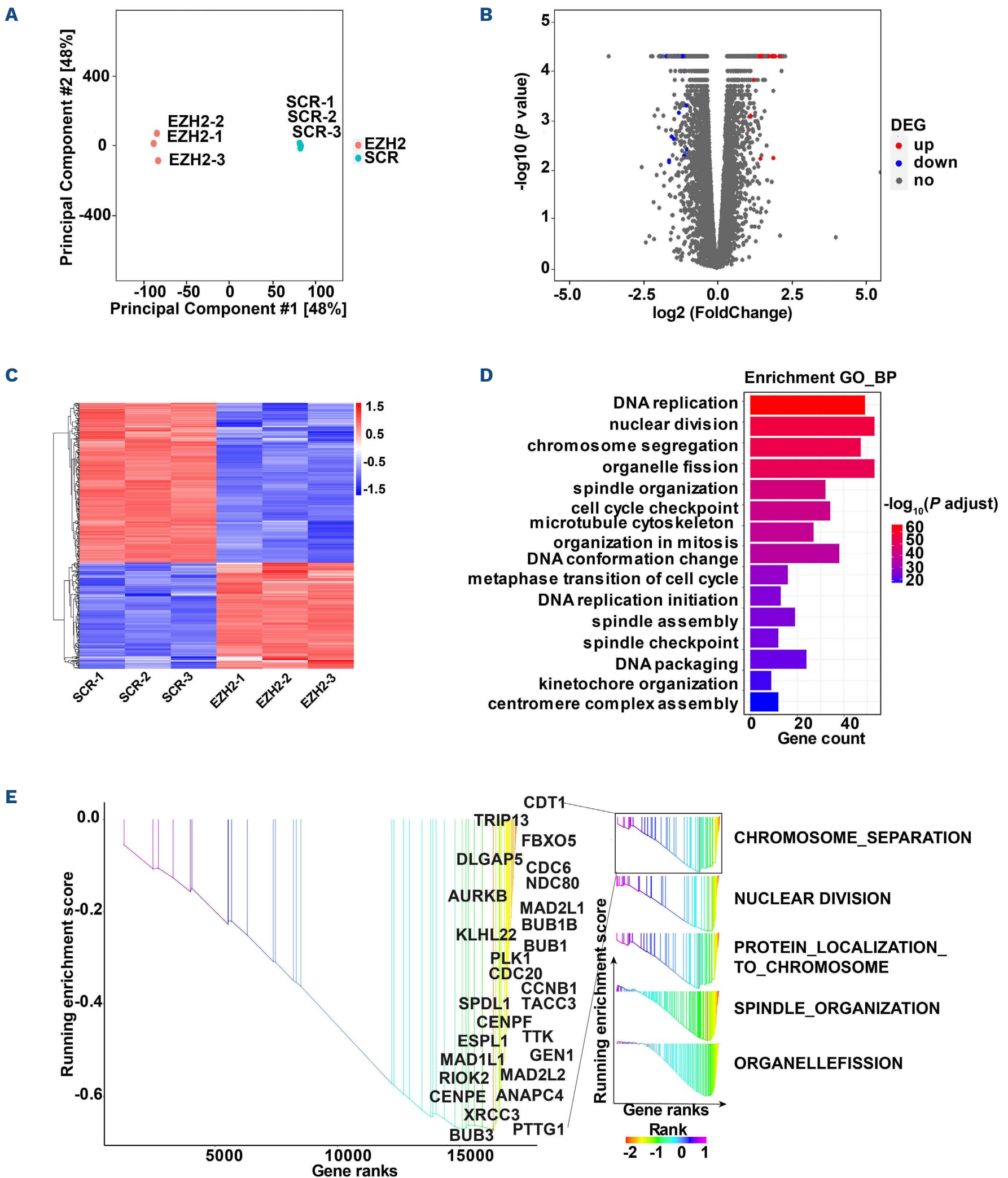


Figure 6. EZH2 deficiency resulted in the downregulation of *AURKB* at transcriptional level. (A) Principal component analysis of samples representing 3 biologic replicates from D15 cells transfected with scramble-small hairpin RNA (shRNA) and EZH2-shRNA. (B) Volcano map showing genes with significant difference between scramble-shRNA and EZH2-shRNA group. (C) Heat map showing expression values of differentially expressed genes (DEG) between scramble-shRNA and EZH2-shRNA group. (D) The top 15 downregulated pathways revealed by gene ontology gene ontology (GO) analysis of the differentially expressed genes between scramble-shRNA and EZH2-shRNA. (E) Rank-based gene set enrichment pathways by EZH2 significantly regulated. The images of gene set enrichment analysis demonstrated the key pathways which all involved in the *AURKB* gene.

Discussion

In this study, we are surprised to find that EZH2 regulates human erythropoiesis in a stage-specific dual function manner, by regulating early erythroid development via catalyzing H3K27me3 and modulating terminal stage development by eliciting non-histone methylation. It is important to note that terminal erythroid differentiation is a complex and highly regulated process that includes decreased nuclear size, chromatin condensation, and culminates in enucleation.^{31,32} Previous studies have shown that some nuclear proteins, such as histones, are exported from the erythroid precursor nucleus into the cytoplasm and ultimately degraded during terminal erythroid development.³⁵ Our results demonstrated that H3K27me3 was exported into the cytoplasm of normal erythroblasts during maturation, whereas EZH2 was constantly localized in the nucleus during normal erythropoiesis. This finding provides a useful model to study the non-canonical roles of EZH2, such as non-histone

methylation, without interference from the classical substrate H3K27me3.

It has been reported that EZH2 deletion can affect cell proliferation through cell cycle arrest in lung cancer cells,³⁶ mouse osteogenesis,³⁷ breast cancer,³⁷ and human glioma cells.³⁷ Trivai et al. also reported that EZH2 abnormalities can promote clonal proliferation of tumorigenic hematopoietic stem cells, block the hematopoietic progenitor cell cycle, and impair erythropoiesis in PMF¹⁵. In our study, on early erythroid development, we found deficiency of EZH2 impaired cell proliferation due to cell cycle arrest in the G1 phase and delayed the differentiation of progenitor erythroid cells. Furthermore, we found that EZH2 function was dependent on H3K27me3 during early erythroid development. A previous study reported that in acute myeloid leukemia, EZH2 deletion leads to a significant reduction in the level of H3K27me3 and affects CDK1 and genes related to the development and differentiation process.³⁸ Consistent with the previous findings, our current study demonstrated that knockdown of EZH2 led to

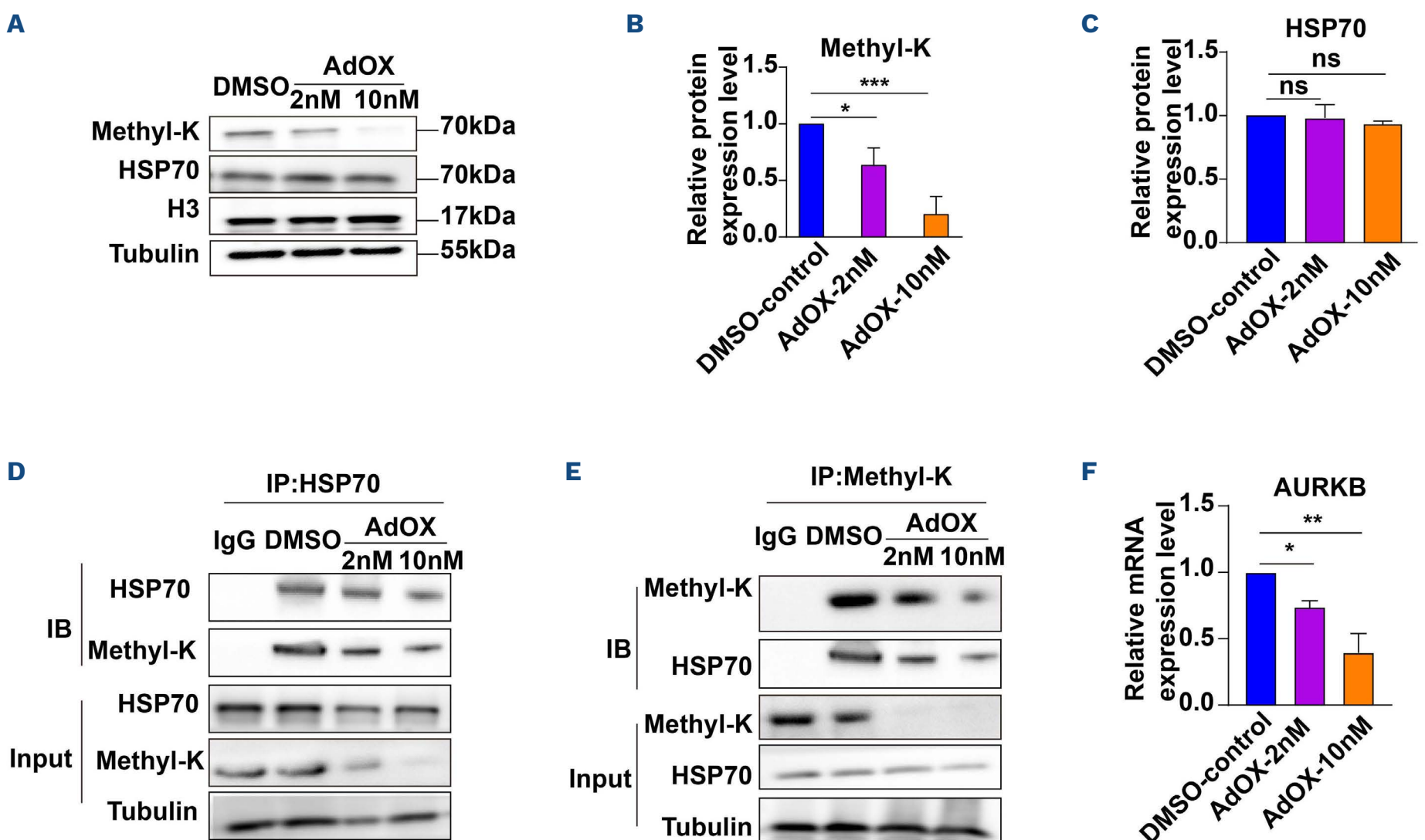


Figure 7. Methylated HSP70 regulates the transcription of AURKB. (A) Representative western blot showing the protein level of HSP70 in cells treated with or without adenosine-2 β , 3 β -dialdehyde (AdOX). H3 and tubulin were used as loading control. (B) Quantitative analysis of the relative protein level of Methyl-K from 3 independent experiments. (C) Quantitative analysis of the relative protein level of HSP70 from 3 independent experiments. (D, E) Cells were treated with or without AdOX (2 nM, 10 nM) and then used in an immunoprecipitation with anti-HSP70 or anti-Methyl-K followed by immunoblotting with anti-Methyl-K or HSP70. (F) Quantitative analysis the relative mRNA expression level of *AURKB* from 3 independent experiments. Statistical analysis is from 3 independent experiments, and the bar plot represents mean \pm standard deviation of triplicate samples. ns: not significant; * P <0.05, ** P <0.01, *** P <0.001. IB: immunoblotting; IP: immunoprecipitation; IgG: immunoglobulin G; DMSO: dimethyl sulf-

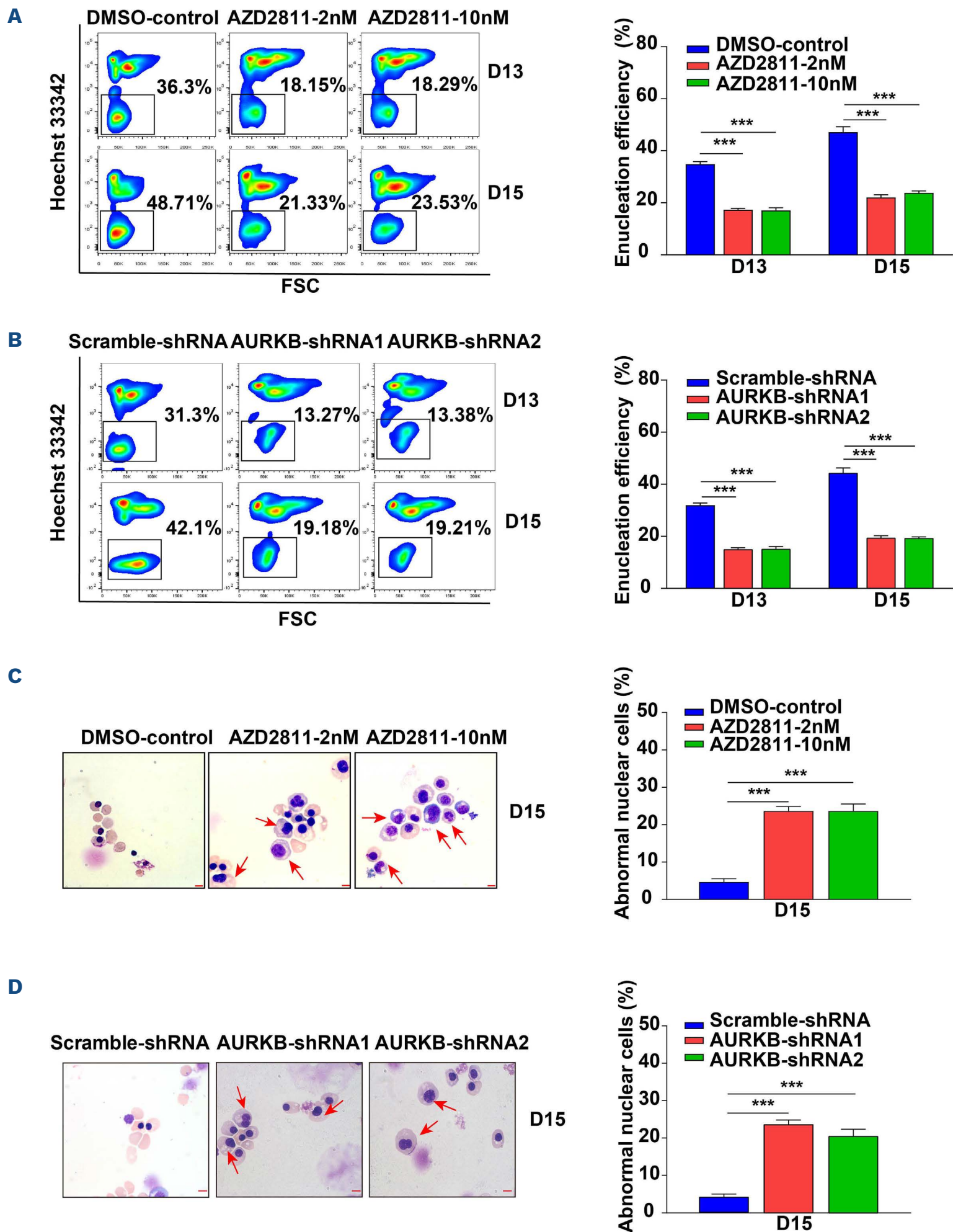


Figure 8. Deficiency of AURKB led to the generation of abnormal nucleus and decreased enucleation efficiency. (A) Flow cytometry analysis showing the enucleation efficiency of dimethyl sulfoxide (DMSO) control, AZD2811 2 nM, and AZD2811 10 nM on days 13 and 15. Statistical analysis of the enucleation efficiency from 3 independent experiments. (B) Flow cytometry analysis showing the enucleation efficiency of scramble-small hairpin RNA (shRNA), AURKB-shRNA1, and AURKB-shRNA2 on days 13 and 15. Statistical analysis of the enucleation efficiency from 3 independent experiments. (C) Representative cytopsin images of DMSO control, AZD2811 2 nM, and AZD2811 10 nM on day 15. Red arrow pointed to cells with abnormal nuclear morphology; scale bar, 5 μ m. Statistical analysis of abnormal nuclear cells from 3 independent experiments. (D) Representative cytopsin images of scramble-shRNA, AURKB-shRNA1, and AURKB-shRNA2 on day 15. Red arrow pointed to cells with abnormal nuclear morphology; scale bar, 5 μ m. Statistical analysis of abnormal nuclear cells from 3 independent experiments. Statistical analysis is from 3 independent experiments, and the bar plot represents mean \pm standard deviation of triplicate samples. ns: not significant; * P <0.05, ** P <0.01, *** P <0.001.

upregulation of cell cycle-related gene expression, including CDKN1A and CDKN1C.

In recent years, it has been shown that EZH2 not only regulates biological processes via catalyzing H3K27me3, but also modulates the transcriptional expression of genes independent of H3K27me3. Numerous studies have shown that EZH2 can modulate non-histone protein methylation in an H3K27me3-independent manner, and most of them are transcription factors (TF) and chromatin-associated proteins,²⁹ such as STAT3,³⁹ GATA4,²⁹ and AR.⁴⁰ Interestingly, during terminal erythroid development, we found in the present study that EZH2 knockdown had no significant effect on the proliferation, apoptosis, and differentiation, but it rather increased abnormal nuclear cells and decreased enucleation efficiency in an H3K27me3-independent manner. We found that H3K27me3 was released into the cytoplasm, while EZH2 was still in the nucleus in the late erythroid cells. Moreover, EZH2 can interact with non-histone HSP70 and HSP90. It is worth mentioning that EZH2 can only regulate HSP70 methylation. Based on these results, we conclude that the dysfunction of the late-stage cells induced by EZH2 knockdown is caused by decreasing non-histone HSP70 methylation independent of the effects of H3K27me3 on terminal erythropoiesis.

HSP70 proteins are well-known molecular chaperones involved in protein folding.^{41,42} Several studies have demonstrated that HSP70 can play an important regulatory role in human erythroblasts by stabilizing GATA1, a core transcription factor in the differentiation and maturation of erythroblasts.²⁴ In our study, the result showed that although knockdown EZH2 significantly affected the methylation of HSP70, but did not affect the protein expression level of HSP70. Based on this finding, we speculated that it is very likely GATA1 is not changed in EZH2-knockdown cells. This hypothesis is supported by our western blot as well as RNA-seq analysis (*Online Supplementary Figure S13A-C*). It has also been reported that abnormal expression or function of HSP70 can promote ineffective erythropoiesis in β -thalassemia,^{43,44} MDS,^{23,45} and Diamond-Blackfan anemia.^{24,46} In addition, an increasing number of studies have revealed other functions of HSP70 chaperone proteins and linked the methylation of non-histone proteins to the regulation of gene transcription.^{33,47} More importantly, a previous study reported that nuclear HSP70 can directly interact with AURKB, and enhanced HSP70 lysine methylation can promote its activity.⁴⁸ In the present study, we provide evidence showing that dysregulation of HSP70 methylation led to repression of AURKB expression during terminal erythroid development.

AURKB has been identified as a key component of chro-

somosome passenger complex (CPC), and inhibition of AURKB leads to impaired CPC function.⁴⁹ The highly dynamic CPC is critical for various cell processes, such as chromatin condensation, chromosome orientation at the mitotic spindle and spindle assembly checkpoints, and cytoplasmic division.⁵⁰ Most of these cell processes have been shown to play critical roles during the unique cell events of the terminal stage of erythropoiesis, including nuclear condensation and enucleation.

In summary, we uncovered a previously unknown mechanistic roles for EZH2 in the regulation of human erythropoiesis. We demonstrated that EZH2 can modulate normal erythropoiesis via catalyzing methylation of both non-histone and histone proteins in a stage-dependent manner. Our findings provide novel insights into understanding of the roles of EZH2 in the regulation of normal and ineffective erythropoiesis.

Disclosures

No conflicts of interest to disclose.

Contributions

XA and LC designed the overall project, analyzed the results and prepared the manuscript, with input from all co-authors. ML, DL and FX performed the experiments with assistance from QY, LS, XW and TW. HCZ performed the integrated bioinformatics analysis with assistance from XQ, JL, HZZ and QK.

Acknowledgments

The authors would like to thank LetPub (www.letpub.com) for linguistic assistance and presubmission expert review.

Funding

This work was supported, in part, by grants from the Natural Science Foundation of China (82170116, 81870094, 81870093, 81900112 and 82000121), the Program for Science & Technology Innovation Talents in Universities of Henan Province (20HASTIT039), the Key Scientific and Technological Research Projects in Henan Province (222102310012) and 2021 science and technology development plan of the Henan Province (212102310037).

Data-sharing statement

Data and materials supporting the findings are available from the corresponding authors upon request. All datasets analyzed in this study are available in the GEO repository at NCBI. The accession number is GSE222115. All other relevant data supporting the key findings of this study are available within the article and its Online Supplementary Appendix.

References

- Hu J, Liu J, Xue F, et al. Isolation and functional characterization of human erythroblasts at distinct stages: implications for understanding of normal and disordered erythropoiesis in vivo. *Blood*. 2013;121(16):3246-3253.
- Chen K, Liu J, Heck S, Chasis JA, An X, Mohandas N. Resolving the distinct stages in erythroid differentiation based on dynamic changes in membrane protein expression during erythropoiesis. *Proc Natl Acad Sci U S A*. 2009;106(41):17413-17418.
- Hewitt KJ, Sanalkumar R, Johnson KD, Keles S, Bresnick EH. Epigenetic and genetic mechanisms in red cell biology. *Curr Opin Hematol*. 2014;21(3):155-164.
- Morgan MAJ, Shilatifard A. Reevaluating the roles of histone-modifying enzymes and their associated chromatin modifications in transcriptional regulation. *Nat Genet*. 2020;52(12):1271-1281.
- Kamminga LM, Bystrykh LV, de Boer A, et al. The Polycomb group gene *Ezh2* prevents hematopoietic stem cell exhaustion. *Blood*. 2006;107(5):2170-2179.
- Ezhkova E, Pasolli HA, Parker JS, et al. *Ezh2* orchestrates gene expression for the stepwise differentiation of tissue-specific stem cells. *Cell*. 2009;136(6):1122-1135.
- Mochizuki-Kashio M, Mishima Y, Miyagi S, et al. Dependency on the polycomb gene *Ezh2* distinguishes fetal from adult hematopoietic stem cells. *Blood*. 2011;118(25):6553-6561.
- Herrera-Merchan A, Arranz L, Ligos JM, de Molina A, Dominguez O, Gonzalez S. Ectopic expression of the histone methyltransferase *Ezh2* in haematopoietic stem cells causes myeloproliferative disease. *Nat Commun*. 2011;3:623.
- Xie H, Xu J, Hsu JH, et al. Polycomb repressive complex 2 regulates normal hematopoietic stem cell function in a developmental-stage-specific manner. *Cell Stem Cell*. 2014;14(1):68-80.
- Kheradmand Kia S, Solaimani Kartalaei P, Farahbakhshian E, Pourfarzad F, von Lindern M, Verrijzer CP. EZH2-dependent chromatin looping controls *INK4a* and *INK4b*, but not *ARF*, during human progenitor cell differentiation and cellular senescence. *Epigenetics Chromatin*. 2009;2(1):16.
- Kamminga LM, Bystrykh LV, de Boer A, et al. The Polycomb group gene *Ezh2* prevents hematopoietic stem cell exhaustion. *Blood*. 2006;107(5):2170-2179.
- Mochizuki-Kashio M, Aoyama K SG, Oshima M, et al. *Ezh2* loss in hematopoietic stem cells predisposes mice to develop heterogeneous malignancies in an *Ezh1*-dependent manner. *Blood*. 2015;126(10):1172-1183.
- Aoyama K, Shinoda D, Suzuki E, et al. PRC2 insufficiency causes p53-dependent dyserythropoiesis in myelodysplastic syndrome. *Leukemia*. 2021;35(4):1156-1165.
- Hu P, Nebreda AR, Hanenberg H, et al. P38alpha/JNK signaling restrains erythropoiesis by suppressing *Ezh2*-mediated epigenetic silencing of *Bim*. *Nat Commun*. 2018;9(1):3518.
- Trivai I, Zeschke S, Rentel J, et al. ASXL1/EZH2 mutations promote clonal expansion of neoplastic HSC and impair erythropoiesis in PMF. *Leukemia*. 2019;31(1):99-109.
- Ernst T, Chase AJ, Score J, et al. Inactivating mutations of the histone methyltransferase gene *EZH2* in myeloid disorders. *Nat Genet*. 2010;42(8):722-726.
- Stasik S, Middeke JM, Kramer M, et al. *EZH2* mutations and impact on clinical outcome: an analysis in 1,604 patients with newly diagnosed acute myeloid leukemia. *Haematologica*. 2020;105(5):e228-e231.
- Vardiman JW, Thiele J, Arber DA, et al. The 2008 revision of the World Health Organization (WHO) classification of myeloid neoplasms and acute leukemia: rationale and important changes. *Blood*. 2009;114(5):937-951.
- Yan H, Wang Y, Qu X, et al. Distinct roles for TET family proteins in regulating human erythropoiesis. *Blood*. 2017;129(14):2002-2012.
- Kim W, Bird GH, Neff T, et al. Targeted disruption of the EZH2-EED complex inhibits EZH2-dependent cancer. *Nat Chem Biol*. 2013;9(10):643-650.
- Perez-Riverol Y, Bai J, Bandla C, et al. The PRIDE database resources in 2022: a hub for mass spectrometry-based proteomics evidences. *Nucleic Acids Res*. 2022;50(D1):D543-D552.
- An X, Schulz VP, Li J, et al. Global transcriptome analyses of human and murine terminal erythroid differentiation. *Blood*. 2014;123(22):3466-3477.
- Frisan E, Vandekerckhove J, de Thonel A, et al. Defective nuclear localization of Hsp70 is associated with dyserythropoiesis and GATA-1 cleavage in myelodysplastic syndromes. *Blood*. 2012;119(6):1532-1542.
- Rio S, Gastou M, Karboul N, et al. Regulation of globin-heme balance in Diamond-Blackfan anemia by HSP70/GATA1. *Blood*. 2019;133(12):1358-1370.
- Kampinga HH, Craig EA. The HSP70 chaperone machinery: J proteins as drivers of functional specificity. *Nat Rev Mol Cell Biol*. 2010;11(8):579-592.
- Schopf FH, Biebl MM, Buchner J. The HSP90 chaperone machinery. *Nat Rev Mol Cell Biol*. 2017;18(6):345-360.
- Hahn JS. The Hsp90 chaperone machinery: from structure to drug development. *BMB Rep*. 2009;42(10):623-630.
- Lee JM, Lee JS, Kim H, et al. EZH2 generates a methyl degron that is recognized by the DCAF1/DDB1/CUL4 E3 ubiquitin ligase complex. *Mol Cell*. 2012;48(4):572-586.
- He A, Shen X, Ma Q, et al. PRC2 directly methylates GATA4 and represses its transcriptional activity. *Gen Dev*. 2012;26(1):37-42.
- Zhao B, Liu H, Mei Y, et al. Disruption of erythroid nuclear opening and histone release in myelodysplastic syndromes. *Cancer Med*. 2019;8(3):1169-1174.
- Ji P, Murata-Hori M, Lodish HF. Formation of mammalian erythrocytes: chromatin condensation and enucleation. *Trend Cell Biol* 2011;21(7):409-415.
- An C, Huang Y, Li M, et al. Vesicular formation regulated by ERK/MAPK pathway mediates human erythroblast enucleation. *Blood Adv*. 2021;5(22):4648-4661.
- Gao WW, Xiao RQ, Peng BL, et al. Arginine methylation of HSP70 regulates retinoid acid-mediated RARβ2 gene activation. *Proc Natl Acad Sci U S A*. 2015;112(26):E3327-3336.
- Harding SM, Benci JL, Irianto J, Discher DE, Minn AJ, Greenberg RA. Mitotic progression following DNA damage enables pattern recognition within micronuclei. *Nature*. 2017;548(7668):466-470.
- Zhao B, Mei Y, Schipma MJ, et al. Nuclear condensation during mouse erythropoiesis requires Caspase-3-mediated nuclear opening. *Dev Cell*. 2016;36(5):498-510.
- Li HS, Xu Y. Inhibition of EZH2 via the STAT3/HOTAIR signalling axis contributes to cell cycle arrest and apoptosis induced by polyphyllin I in human non-small cell lung cancer cells. *Steroids*. 2020;164:108729.
- Dudakovic A, Camilleri ET, Paradise CR, et al. Enhancer of zeste homolog 2 (*Ezh2*) controls bone formation and cell cycle progression during osteogenesis in mice. *J Biol Chem*. 2018;293(33):12894-12907.
- Tanaka S, Miyagi S, Sashida G, et al. *Ezh2* augments leukemogenicity by reinforcing differentiation blockage in acute

- myeloid leukemia. *Blood*. 2012;120(5):1107-1117.
39. Kim E, Kim M, Woo DH, et al. Phosphorylation of EZH2 activates STAT3 signaling via STAT3 methylation and promotes tumorigenicity of glioblastoma stem-like cells. *Cancer Cell*. 2013;23(6):839-852.
40. Xu K, Wu ZJ, Groner AC, et al. EZH2 oncogenic activity in castration-resistant prostate cancer cells is Polycomb-independent. *Science*. 2012;338(6113):1465-1469.
41. Imamoglu R, Balchin D, Hayer-Hartl M, Hartl FU. Bacterial Hsp70 resolves misfolded states and accelerates productive folding of a multi-domain protein. *Nat Commun*. 2020;11(1):365.
42. Polier S, Dragovic Z, Hartl FU, Bracher A. Structural basis for the cooperation of Hsp70 and Hsp110 chaperones in protein folding. *Cell*. 2008;133(6):1068-1079.
43. Arlet JB, Ribeil JA, Guillem F, Hermine O, Courtois G. HSP70 regulates ineffective erythropoiesis in beta-thalassaemia. *Med Sci (Paris)*. 2015;31(1):9-11.
44. Hermine O, Arlet JB, Ribeil JA, Guillermin F, Vandekerckhove J, Courtois G. HSP70, an erythropoiesis regulator that determines the fate of erythroblasts between death and differentiation. *Transfus Clin Biol*. 2013;20(2):144-147.
45. Dong XM, Zhao K, Zheng WW, et al. EDAG mediates Hsp70 nuclear localization in erythroblasts and rescues dyserythropoiesis in myelodysplastic syndrome. *FASEB J*. 2020;34(6):8416-8427.
46. Gastou M, Rio S, Dussiot M, et al. The severe phenotype of Diamond-Blackfan anemia is modulated by heat shock protein 70. *Blood Adv*. 2017;1(22):1959-1976.
47. Wang J, Wang GG. No easy way Out for EZH2: its pleiotropic, noncanonical effects on gene regulation and cellular function. *Int J Mol Sci*. 2020;21(24):9501.
48. Cho HS, Shimazu T, Toyokawa G, et al. Enhanced HSP70 lysine methylation promotes proliferation of cancer cells through activation of Aurora kinase B. *Nat Commun*. 2012;3:1072.
49. Adams RR, Carmena M, Earnshaw WC. Chromosomal passengers and the (aurora) ABCs of mitosis. *Trends Cell Biol*. 2001;11(2):49-54.
50. Petsalaki E, Zachos G. The abscission checkpoint: a guardian of chromosomal stability. *Cells*. 2021;10(12):3350.